Chapter 31

Small-Angle Scattering from Long-Chain Alkylimidazolium-Based Ionic Liquids

C. Hardacre[1], J. D. Holbrey[1,2], S. E. J. McMath[1], and M. Nieuwenhuyzen[1]

[1]School of Chemistry and the QUILL Centre, The Queen's University of Belfast, Stranmillis Road, Belfast BT9 5AG, Northern Ireland, United Kingdom
[2]Current address: Center for Green Manufacturing, The University of Alabama, Tuscaloosa, AL 35487

This paper compares the structure of 1-alkyl-3-methylimidazolium salts using SAXS and X-ray reflectivity. A range of anions have been investigated namely chloride, bromide, trifluoromethanesulfonate (OTf), *bis*(trifluoromethanesulfonyl)imide (TFI) and tetrachloropalladate(II) with cation alkyl chains ranging from n = 12-20. In general, the salts show liquid crystalline behaviour whose structure is still observed on melting into an isotropic liquid.

Room-temperature ionic liquids have been utilised as clean solvents and catalysts for green chemistry (*1*) and as electrolytes for batteries, photochemistry and electrosynthesis (*2*), each of which have been extensively reviewed. Interest in this class of solvent stems from the properties exhibited by the liquids (including effectively zero vapour pressure) and the ease by which many of their physical properties may be varied (*3*). Currently, the ionic liquids of choice for these applications comprise of an organic cation, for example 1,3-dialkylimidazolium cations (*4*) (Figure 1) with a wide variety of anions (*5-7*). By lengthening one of the alkyl-chain substituents of the 1-alkyl-3-methylimidazolium cation, large changes in the physical properties of the

In Ionic Liquids; Rogers, Robin D., et al.;
ACS Symposium Series; American Chemical Society: Washington, DC, 2002.

resultant ionic liquids can be achieved (*8*). These include changes in viscosity and density as well as the ready formation of thermotropic liquid crystal mesophases (*9*) for long-chain salts. These latter salts resemble those of related *N*- alkylammonium salts previously reported by, for example, Busico *et al.*(*10*).

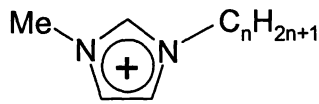

Figure 1 The general structure of 1-alkyl-3-methylimidazolium cation for the salts studied (n = 12-20).

Amphiphilic ionic salts have many applications for example, templating mesoporous materials (*11*), the formation of ordered films (*12*), as ionic liquid crystals (*10,13*) and ionic metallomesogens (*14,15*). In the latter, metal-containing moieties can be introduced as either the mesogenic unit (*16*) or as the counter ion.(*17,18*)

In this paper, we present SAXS and X-ray reflectivity data for a range of 1-alkyl-3-methylimidazolium salts with chloride, bromide, trifluoromethanesulfonate (OTf), *bis*(trifluoromethanesulfonyl)imide (TFI) and tetrachloropalladate(II) anions. The structure of the salts described are compared and show a common motif in both the crystal and liquid crystalline phases which, in the latter case, is still present in the liquid structure.

Experimental

The salts were prepared from the corresponding 1-alkyl-3-methylimidazolium chloride salts by metathesis using established literature procedures (*5-8*). Each salt was purified by recrystallisation and characterised by elemental analysis, ^{1}H and ^{13}C NMR spectroscopy and differential scanning calorimetry (DSC). In each case the purity was greater than 99.5% estimated from elemental analysis. The melting points, DSC traces and polarizing optical microscopy for each salt studied is detailed in references 5 and 20.

Variable temperature small angle X-ray scattering (SAXS) experiments were carried out at the SRS, Daresbury, UK on beamline 8.2. Data were obtained from the salts in sealed 1 mm glass Lindemann tubes using a monochromated (1.54 Å) X-ray beam. Samples were transferred to the Lindemann tubes as molten liquids. A multiwire quadrant detector was used with camera length of 0.95 m, effective range 8 - 190 Å. Heating was achieved using a Linkam hot stage. The detector was calibrated with silver behenate(*19*).

The X-ray reflectivity experiments were carried out at the SRS in Daresbury, U.K., on station 16.2. The X-ray beam was monochromated to 1.36 Å and data was collected over the incidence angle range 0-5°. Samples were spin coated from methanol solutions onto cleaned, polished Si(111) wafers In each case, the samples were annealed above the respective melting points of the samples and the measurements taken on the thermally treated films.

The details of the analysis and methods used have been published previously for both the SAXS (*5,20*) and X-ray reflectivity measurements (*21*).

Results

Small Angle X-ray Scattering

Non-metal containing 1-methyl-3-alkyl imidazolium salts.

Figure 2 shows typical SAXS data for the salt [C_{16}-mim][OTf]. This is a specific example of the more general pattern found for all the non-metal salts studied, *i.e.* for Cl^-, Br^-, $[OTf]^-$, $[TFI]^-$ and $[BF_4]^-$. Each of the salts shows at least one peak in the small angle region and diffraction patterns which are consistent with a lamellar structure containing charged layers separated by hydrocarbon chains in both the crystal and liquid crystalline phases. Table 1 summarises the interlayer spacing, *d*, based on the lowest angle feature in the SAXS data on cooling from the liquid phase. The interlayering spacing was calculated using Bragg's law.

For those salts showing a liquid crystalline phase, the SAXS pattern in the mesophase consists of a sharp peak between 2θ = 1–5°, *i.e.* the phase has an interlayer spacing between 22-61 Å. As expected the interlayer spacing increases uniformly with increasing alkyl chain length, *n*, however the variation with anion is more complex. For a given cation the mesophase interlayer spacing decreases following the order Cl^- > Br^- > $[BF_4]^-$ > $[OTf]^-$ with the *bis*(trifyl)imide salts not exhibiting any mesophase structure.

In the crystal phase, the SAXS data contains more features. In general, more than one phase is displayed but this is highly dependant on the thermal history of the samples. In the majority of the non-metal salts studied, an intense

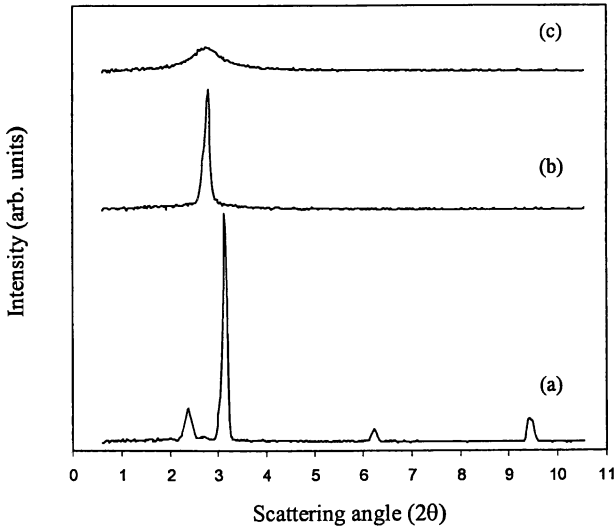

Figure 2 SAXS pattern for [C_{16}-mim][OTf] at (a) 50 °C, (b) 70 °C and (c) 90 °C, in the crystal, SmA_2 and isotropic phases respectively, on cooling.

feature is displayed between 2θ = 2.8–3.9°. Taking this feature as the (001) interlayer repeat, on transforming from the crystal to the mesophase, the interlayer spacing increases for all the salts studied. This is clearly shown in Figure 2(a) and (b), where the (001) peak is shifted from 3.12 ° to 2.79° with increasing temperature, corresponding to a increase in the interlayer spacing from 28.2 Å in the crystal phase to 31.6 Å in the mesophase. This is not unusual for surfactants molecules.

Some of the salts, specifically those containing halide, also exhibit SAXS peaks below 2°. This is illustrated in Figure 3 for [C_{18} -mim]Cl. In this case, an intense peak is observed at 1.45° corresponding to a *d* spacing of 60.9 Å. However, the presence of the large interlayer spacing is not reversible, after one heating-cooling cycle the feature disappears and is replaced by a single feature at 2.85° (*d* = 31.0 Å) in line with the diffraction patterns for the other salts.

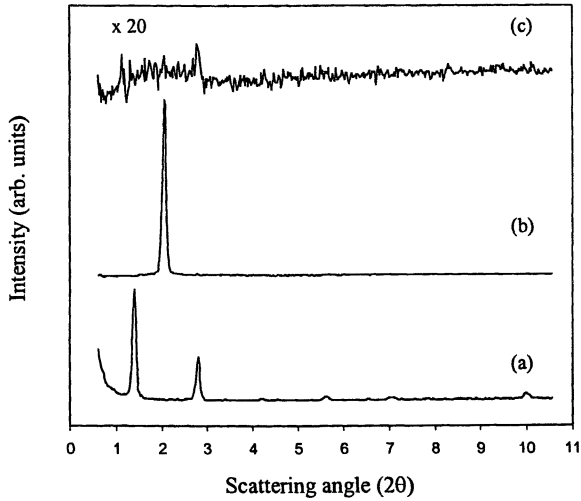

Figure 3 SAXS pattern for [C_{18}-mim]Cl at (a) 30 °C, (b) 75 °C and (c) cooled back to 30 °C, i.e. in the crystal, liquid crystal and back to the crystal phases, respectively.

For all the non-metal salts studied, the SAXS data also shows smaller features in the crystal phase. For example, in Figure 2, peaks are observed at 2.45°, corresponding to a periodicity of 36.0 Å, and in the wider angle data at 9.40°, corresponding to 9.4 Å. In all cases, these peaks are much less intense and do not fit the regular repeat unit of the layered structure (determined from the (001) and (002) peaks at 2θ = 3.15° and 6.30°, respectively). The wider angle feature corresponds to the cation–cation and anion–anion repeat distance within the charged region. This feature is only present in the initial crystal structure, on cooling from the liquid phase, the peak disappears indicative of a reduction in the positional ordering within the layer.

On melting to the isotropic liquid, a broad peak is observed in the SAXS data for each salt. This peak indicates that even within the isotropic liquid phase, some short-range associative structural ordering is still retained.

Palladium containing 1-methyl-3-alkyl imidazolium salts.

For the palladium containing salts, the SAXS data for all alkyl chain lengths studied showed similar patterns consistent with a layered structure as observed for the non-metal containing salts. Table 1 also summarises the interlayer spacings found for the palladium based salts.

In the room temperature crystal phase, peaks are observed at low angle, 2θ = 1.58–1.87°. These correspond to (001) interlayer spacings of between 47-

Table 1 Summary of (001) interlayer(d / Å) spacings determined from SAXS data, based on the lowest angle scattering peak.

n	*Anion*	*Phase*			
		Crystal			*Liquid Crystal*
12	$[TFI]^-$	24.7			-
14		25.2			-
16		28.2			-
18		28.8			-
12	$[OTf]^-$	26.8			-
14		29.4			-
16		28.2 (36.6[a])			31.7
18		30.3 (43.4[a])			34.4
12	$[BF_4]^-$	-			-
14		27.2			31.4
15		28.6			33.0
16		32.1			35.4
18		34.6			37.7
12	Cl^-	22.5	-		31.7
14		50.7[b]	25.8		34.4
16		56.6[b]	29.0		36.6
18		60.9[b]	31.0		41.2
12	Br^-	22.8	-		32.0
14		53.5[b]	27.0		33.6
16		30.7	-		36.3
20		31.6	-		38.8
12	$[PdCl_4]^{2-}$	47.1[b]	31.9	33.0	-
14		50.1[b]	35.2	37.2	30.3
16		55.8[b]	37.6	39.9	33.2
18		-	41.1	43.4	35.4

[a]low intensity peak associated with periodicity along the alkyl chain director.

[b]initial crystal phase observed on first heating only.

56 Å. Figure 4 shows the variation in the SAXS pattern with temperature for $[C_{14}\text{-mim}]_2[PdCl_4]$ as a typical example. In this pattern, two other peaks are shown, the second order diffraction peak at 3.52° and a weaker peak at *ca.* 8.25°, which corresponds to a periodicity of 10.6 Å. The latter is associated with the $[PdCl_4]^{2-}$ to $[PdCl_4]^{2-}$ anion correlation distance.(*17*,22)

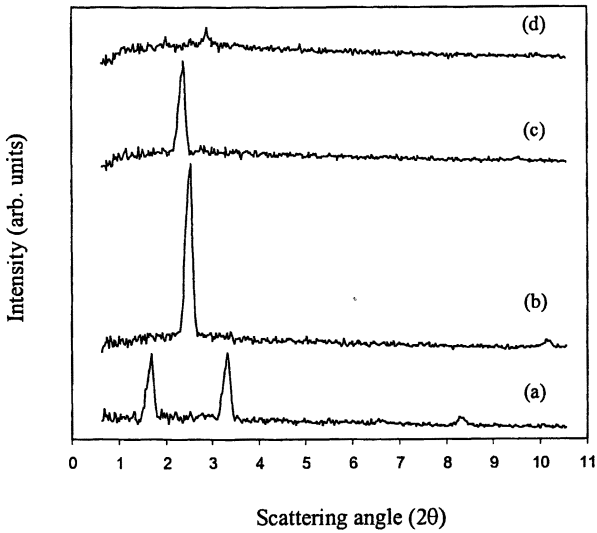

Figure 4 SAXS pattern for $[C_{14}\text{-mim}]_2[PdCl_4]$ at (a) 50 °C, (b) 85 °C and (c) 110 °C and (d) 140 °C from first heating.
(Reproduced with permission from reference 5. Copyright 2001 Taylor & Francis.)

On heating $[C_{14}\text{-mim}]_2[PdCl_4]$ to 78 °C, an irreversible phase change occurs from Cr to a higher temperature Cr' phase. In the Cr' phase, the low angle feature disappears and a single peak is observed at 2.51°, corresponding to a (001) layer spacing of 35.2 Å. A shift to higher angle is also observed in the wide angle features, corresponding to a decrease in the anion-anion correlation from 10.6 Å to 8.7 Å.

At 100 °C, the salt undergoes a second crystal-crystal transition to a Cr" phase, indicated by a small shift in the (001) peak to lower angle. In Figure 4, the peak shifts from 2.51° to 2.37°, *i.e.* an increase in the (001) layer spacing from 35.2Å to 37.2 Å. For all the palladium salts studied, transforming from the Cr' to Cr" phase results in the loss of the higher angle reflection associated with the anion-anion correlation.

Above 120 °C, the Cr" phase melts to a liquid crystalline phase with the (001) peak shifting to higher angle due to a contraction of the interlayer spacing. For $[C_{14}\text{-mim}]_2[PdCl_4]$, the interlayer spacing decreases from 37.2 to 30.3 Å.

This phase change is accompanied by a marked decrease in intensity and broadening of the (001) peak. No liquid crystalline phase was observed for $[C_{12}\text{-mim}]_2[PdCl_4]$.

The latter two phase transitions (*i.e.* Cr'-Cr" and Cr"-liquid crystal) are fully reversible on cooling. However, in all cases the structure remains in the Cr' phase on cooling.

X-Ray Reflectivity

Table 2 summarises the X-reflectivity data exhibited by palladium containing and non-metal long alkyl chain imidazolium salts. In each cases, the periodicity data extracted from patterns is derived from thermally treated films. The untreated spin coated samples showed a featureless profile due to the films being rough. After melting to the liquid and cooling, smooth ordered films were produced with thickness ranging from 100-210 Å as determined from the minimum in Q_z. For all the salts studied, Bragg features were clearly visible, however, in most cases, the additional Kiessig fringes which allow the structure within the film and at the interfaces to be determined were not evident. The Bragg peaks indicate an ordered local structure within the sample film and the interlayer spacings, determined from the position of the first Bragg peak, are given for the solid and liquid crystalline films.

For each salt, the films have periodicities which are similar to those found for the bulk samples. In general, the films exhibit a slightly larger distance than in the bulk samples, for example $[C_{18}\text{-mim}][PF_6]$ reflectivity gives 29.5 Å whereas 27.7 Å is determined from X-ray diffraction on the bulk sample. It should be noted that in the case of the $[C_{12}\text{-mim}]_2[PdCl_4]$ film, the long range periodicity observed in the SAXS data is not observed in the thin films due to the samples being thermally treated and this initial transition was only observed in the SAXS for the untreated sample. In this sample, two Bragg features were observed on cooling through the intermediate crystal phase from the isotropic liquid to the room temperature crystal phase corresponding to a mixed phase of two crystal phases with periodicities of 30.7 Å and 33.1 Å. The latter corresponds to the low temperature phase and has a periodic spacing greater than that for the thermally treated bulk samples, *i.e.* in the Cr' phase.

For the $[PF_6]^-$ and $[BF_4]^-$ films, the liquid crystalline phases show an increased layer spacing compared with the solid as was observed in the SAXS data.

Kiessig fringes were observed in addition to the Bragg feature for the $[C_{18}\text{-mim}][PF_6]$ salt. These were present in both liquid crystalline and solid phases, however, they were more pronounced in the latter. The details of the Kiessig fringes is beyond the scope of this paper but is presented in reference 21, an example of the data obtained is shown in Figure 5

Table 2 Summary of interlayer (d / Å) spacings determined from X-ray reflectivity data, based on the lowest Bragg peak.

n	*Anion*	*Phase*		
		Crystal[a]	*Liquid Crystal*	*Bulk Crystal*[b]
18	$[BF_4]^-$	34.7	36.5	34.6
12	$[PdCl_4]^{2-}$	33.1 / 30.7	31.8[c]	31.9
12	$[PF_6]^-$	23.4	-	22.4
18		29.5	34.5	27.7

[a]Thermally treated films, pre-melted prior to measurement.

[b]Determined from SAXS and XRD data on salt crystallized from the melt.

[c]Crystal-crystal transition, no liquid crystalline phase present.

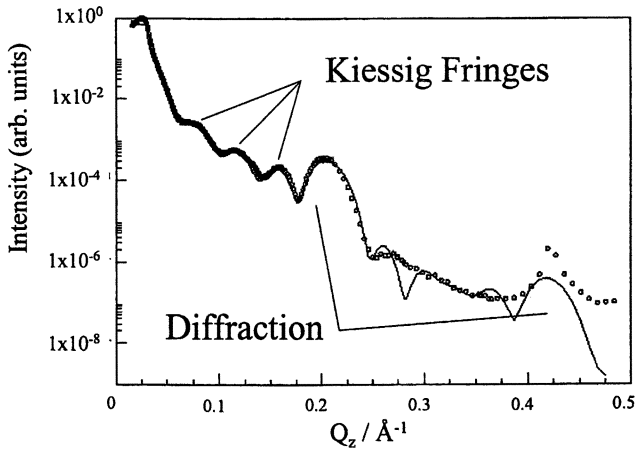

Figure 5 Experimental reflectivity data (points) compared with a 5 bilayer model (solid line) for a 156 Å thick [C_{18}-mim][PF_6] films at 298 K. . (Reproduced with permission from reference 21. Copyright 2001.)

Discussion

The structure of all the salts studied are similar and consist of charged layers of anions and cations separated by regions of alkyl chains consistent with the X-ray single crystal structure of [C_{12}-mim][PF_6] (*6*). In general, the *d* spacings in both the crystal and liquid crystalline phases for all the salts studied lie between *l* and *2l*, where *l* is the fully extended alkyl chain length. This indicates that in both phases, the alkyl-chains of the cations are interdigitated and/or tilted with respect to the layer normal. POM measurements (*5,20*) on all the liquid crystalline phases indicate that there is no angular alignment within the hydrocarbon region consistent with a thermotropic smectic A assignment and thus interdigitation must be present.

The general phenomena that the layer spacing increases, on transforming from the crystal to the mesophase in the non-metal containing crystals, indicates that not only do the alkyl chains melt but the structure also undergoes a conformational change, for example decreasing the angle of tilt with respect to the layer normal. In the palladium containing salts, a decrease in the layer spacing is found on forming the liquid crystalline phase. In this case, if the alkyl chains are tilted, any conformational change is of secondary importance compared with the alkyl-chain melting.

The tetrachloropalladate salts, show crystal polymorphism which is not found at the temperatures studied for the non-metal containing salts, in general. In the palladium salts, the large periodicity found at room temperature is approximately twice the molecular length (*l*) of the fully extended cation (for $n = 14$; $d = 52.1$ Å and $l = 26$ Å, based on molecular models). Two models can be proposed to explain this periodicity,

(i) a lamellar, bilayer structure with no alkyl-chain interdigitation, *i.e.* end to end packing of the alkyl chains or

(ii) a double bilayer structure where the conformations of the head-groups in alternating layers is different.

Although it is not possible to distinguish the two scenarios using the data presented here, it is more likely that the interdigitated structure is formed.

Some crystal polymorphism is also shown by the halide salts. As with the tetrachloropalladate salts, [C_n-mim]Cl ($n = 14, 16, 18$) and [C_{14}-mim]Br show a large periodicity in the room temperature crystal structure. This structure is not stable with respect to temperature and collapses to a much smaller spacing on cooling from the liquid.

In both the halide and tetrachloropalladate salts, these initial crystal structures may be considered as unusual and are due to a solvent induced crystal structure as opposed to ones nucleated from the melt. In this case (i) would simply revert to a structure where interdigitation was present whereas in (ii) the charged region would have similar conformations of the head-groups in

alternating layers. It should be noted that for all salts studied the signal-to-noise on cooling from the liquid or liquid crystalline regions is much reduced, as shown in Figure 3(c). This indicates that the liquid crystal undergoes a glass transitions and although some order is present, it decreases on thermal crystallisation compared with solvent crystallisation.

A layered structure is consistent with the Bragg diffraction found in the thin films as determined by X-ray reflectivity. The gross features are reproduced compared with the bulk samples with only minor shifts in layer spacing. The small changes in layer spacing are likely to be due to the thin film structure not being constrained by long range order effects and hence adopts a slightly different lower energy form. The structure found is likely to be substrate dependant as the orientation of the charged groups on the surface will determine how the molecules pack. The similarity between the bulk samples and the thin film is further exemplified from the modeling of the Kiessig fringes in the case of $[C_{18}\text{-mim}][PF_6]$. Here, the data were modeled using a volume fraction based on the periodic bilayer structure in the crystal structures of long-chain alkylimidazolium salts (*6*) was used. This model was comprised of layers of associated 1-ethyl-3-methylimidazolium cation head groups and hexafluorophosphate anions, denoted as the charged region, separated by hydrocarbon-chains. Reasonable fits were only obtained with the charged region at both the salt-silicon and salt-air interfaces.

The *d* spacing in the mesophase and whether or not a mesophase forms is is determined by the anion-cation interactions within the polar region. In general, the *d* spacing increases $Cl^- > Br^- > [BF_4]^- > [OTf]^- > [TFI]^-$ which follows the anion ability to form hydrogen bonds in a three dimensional lattice. The order may also be determined from the charge density of the anion. However, this simple criterion needs to be qualified since not all the anions looked at are pseudo-spherical, with a total distributed charge density. For example, although the overall charge density for trifluoromethanesulfonate is likely to be lower than for tetrafluoroborate, the charge is localized on the oxygen and therefore the local charge will be higher. It is therefore necessary to add a second argument concerning the accessability of the charge in order to explain the variation observed.

The indication of order in the liquid structure which is similar to that found in the crystal and mesophases allows inferences to made about the liquid stucture packing from the solid state and liquid crystalline data. In this study, it could be argued that the ordering in the liquid is simply a consequence of the long alkyl chains. However, similar results have also been noted for dimethyl imidazolium chloride using neutron scattering (*23*). In this case the crystal structure shows that the chloride is associated with the ring hydrogens of the imidazolium ring and the closest contact between the cations is methyl hydrogen to methyl hydrogen. Although the distances are expanded in the neutron scatteing of the

melt, these features are reproduced in the liquid phase. This order is present out to at least two shells of chloride.

Conclusions

All the diffraction patterns are consistent with a lamellar bilayer structure where the charged species are separated by indigitated and, in general, tilted alkyl chains. In general, the long alkyl chain imidazolium salts form liquid crystalline phases denoted as smectic A, however the interlayer spacings found are dependant on both the alkyl chain length of the cation as well as the anion type. Some polymorphism is found in the crystal phase but this generally only occurs with the tetrachloropalladate anion. For certain halide and tetrachloropalladate salts, solvent induced crystallization results in a metastable phase with a large periodicity. However, this phase irreversibly transforms on heating and the stable thermal induced crystallization fits with the general trends found for all the other salts studied.

Acknowledgements

The authors would like to thank DENI (SEJMcM) for financial support and the EPSRC for SAXS beamtime (Grant GR/M89775).

References

1 Holbrey, J. D.; Seddon, K. R. *Clean Products and Processes* **1999**, *1*, 233; Welton, T. *Chem. Rev.* **1999**, *99*, 2071; Chauvin, Y.; Olivier-Bourbigou, H. *Chemtech* **1996**, *25*, 26; Pagni, R. M. *Adv. Molten Salt Chem.* **1985**, *6*, 211.
2 Hussey, C. L. *Electrochem.* **1999**, *76*, 527; Hussey, C. L. *Pure Appl. Chem.* **1988**, *60*, 1763; Hussey, C. L. *Adv. Molten Salt Chem.* **1983**, *5*, 185.
3 Freemantle, M. *Chem. Eng. News* **1998**, *76*, March 30, 32
4 Wilkes, J. S.; Levisky, J. A.; Wilson, R. A.; Hussey, C. L. *Inorg. Chem.* **1982**, *21*, 1263.
5 Hardacre, C; Holbrey, J. D.; McCormac, P. B.; McMath, S. E. J.; Nieuwenhuzen, M; Seddon, K. R. *J. Mater. Chem.* **2001**, *11*, 346.
6 Gordon, C. M.; Holbrey, J. D.; Kennedy, A. R.; Seddon, K. R. *J. Mater. Chem.* **1998**, *8*, 2627.
7 Bonhôte, P.; Dias, A. P.; Papageorgiou, N.; Kalyanasundaram, K.; Grätzel, M. *Inorg. Chem.* **1996**, 35, 1168..
8 Holbrey, J. D.; Seddon, K. R. *J. Chem. Soc., Dalton Trans.* **1999**, 2133
9 Gray, G. W.; Goodby, J. W. *Smectic Liquid Crystals, Textures and Structures*; Leonard Hill, Glasgow, 1984.

10 Busico, V.; Corradini, P.; Vacatello, M. *J. Phys. Chem.*, **1983**, *87*, 1631; Busico, V.; Corradini, P.; Vacatello, M. *J. Phys. Chem.*, **1983**, *86*, 1033.
11 Huo, Q.; Margolese, D. I.; Ciesla, U.; Feng, P.; Gier, T.; Sleger, P.; Leon, R.; Petroff, P. M.; Schüth, F.; Stucky, G. D. *Nature* **1994**, *368*, 317.
12 Yollner, K.; Popovitz-Biro, R.; Lahau, M.; Milstein, D. *Science* **1997**, *728*, 2100.
13 Abdallah, D. J.; Robertson, A.; Hsu, H.-F.; Weiss, R. G. *J. Amer. Chem. Soc.* **2000**, *122*, 3053.
14 Neve, F. *Advanced Mater.* **1996**, *8*, 277.
15 Hudson, S. A.; Maitlis, P. M. *Chem. Rev.* **1993**, *93*, 861. Bruce, D. W. *J. Chem. Soc., Dalton Trans.* **1993**, 2983. Bruce, D. W. *Metal-containing Liquid Crystals*. In *Inorganic Materials*, 2nd ed., Eds. D. W. Bruce, D. O'Hare, John Wiley & Sons Ltd., 1996; Giroud-Godquin, A. M. *Coord. Chem. Rev.* **1998**, *180*, 1485.
16 Bruce, D. W.; Holbrey, J. D.; Tajbakhsh, A. R.; Tiddy, G. J. T. *J. Mater. Chem.* **1993**, *9*, 905; Holbrey, J. D.; Tiddy, G. J. T.; Bruce, D. W. *J. Chem. Soc., Dalton Trans.* **1995**, 1769; Jervis, H. B.; Raimondi, M. E.; Raja, R.; Maschmeyer, T.; Seddon, J. M.; Bruce, D. W. *J. Chem. Soc., Chem. Commun.* **1999**, 2031.
17 Neve, F.; Crispini, A.; Armentano, S.; Francescangeli, O. *Chem. Mater.* **1998**, *10*, 1904.
18 Bowlas, C. J.; Bruce, D. W.; Seddon, K. R. *J. Chem. Soc., Chem. Commun.*, **1996**, 1625.
19 Huang, T. C.; Toraya, H.; Blanton, T. N.; Wu, Y. *J. Appl. Cryst.* **1993**, 26, 180.
20 Bradley, A. E.; Hardacre, C.; Holbrey, J. D.; Johnston, S.; McMath, S. E. J.; Nieuwenhuyzen, M. *submitted to Chem. Mat.*
21 Carmichael, A. J.; Hardacre, C.; Holbrey, J. D.; Nieuwenhuyzen, M.; Seddon, K. R. *Mol. Phys.*, **2001**, *99*, 795.
22 Neve, F.; Crispini, A.; Francescangeli, O. *Inorg. Chem.*, **2000**, *39*, 1187
23 Bowron, D.T.; Hardacre, C.; Holbrey, J.D.; McMath, S.E.J.; Soper, A.K. *paper in preparation*.